



AC conductivity and dielectric properties of nanostructured amorphous manganese dioxide and polypyrrole/manganese dioxide composite

Yankappa A. Kulakarni¹, M. R. Jagadeesh^{2,*}, Sahebagouda Jambaladinni³, H. M. Suresh Kumar⁴, M. S. Vasanthkumar⁵, and S. Shivakumara^{6,*} 

¹Department of Physics, BLDEA's Vachana Pitamaha Dr. P.G. Halakatti College of Engineering and Technology, Affiliated to Visvesvaraya Technological University, Belgavi, Karnataka 586103, India

²Department of Physics, Jain Institute of Technology, Davangere, Affiliated to Visvesvaraya Technological University, Belgavi, Karnataka 577003, India

³Department of Physics, Government Engineering College, Huvinahadagali, Karnataka 583219, India

⁴Department of Physics, Siddaganga Institute of Technology, Tumakuru, Karnataka 572103, India

⁵Department of Physics, Acharya Institute of Technology, Soladevanahalli, Bangalore, Karnataka 560107, India

⁶Department of Chemistry, REVA University, Kattigenahalli, Yelahanka, Bangalore, Karnataka 560064, India

Received: 2 October 2020

Accepted: 10 December 2020

© The Author(s), under exclusive licence to Springer Science+Business Media, LLC part of Springer Nature 2021

ABSTRACT

Polypyrrole/manganese dioxide (Ppy/MnO₂) nanocomposite has been prepared by a simple in-situ redox reaction between pyrrole monomer and aqueous KMnO₄ solution under ambient conditions. The prepared Ppy/MnO₂ nanocomposite was characterized by powder X-ray diffraction (PXRD), Fourier transformer infrared spectroscopy (FT-IR), scanning electron microscopy (SEM), and AC impedance spectroscopic properties have been studied. PXRD and FT-IR spectral analysis studies reveal that the MnO₂ nanoparticles are embedded in polypyrrole matrix. The electrical conductivity of polypyrrole-based nanocomposite has been reported in the frequency range of 10 Hz to 100 MHz at ambient conditions. The observed behaviour showed that the conductivity of Ppy/MnO₂ nanocomposite increased with increase of frequency.

1 Introduction

Among the available metal oxides, manganese dioxide receives much attraction due to low cost, abundantly availability and relatively non-toxic nature. Manganese dioxide-based materials have been studied for the potential applications in the field of

sensors, electrochemical energy storage and energy conversion devices [1–4]. MnO₂ possesses different crystallographic forms; among these crystallographic forms, α - and δ -MnO₂ are of great interest because of their structural properties [1–4]. However, the performance of these materials is not up to the mark because of their poor conducting nature [1–3]. But the

Address correspondence to E-mail: jmrshyagale@gmail.com; elesk@gmail.com

conducting properties of manganese dioxide are perhaps improved by inclusion of conducting support [6, 7]. There are ample research reports that have been published in the literature to improve the conductance of manganese dioxide using conducting polymer matrix [1–3, 6–8]. Conducting polymer-based metal oxides have been widely studied for electrical and electrochemical applications, in which the polymer chain acts as conducting backbone for the poor conducting metal oxide materials and hence the improved electrical conductivity of nanocomposites [9–18].

It has been proved that polypyrrole acts as a good conducting support by enhancing catalytic property, electrical and electrochemical properties of manganese dioxide [9–14]. Polypyrrole/manganese dioxide nanocomposite electrode materials have been studied for energy storage, sensors and catalysis applications [1–3, 7]. The nanostructured polypyrrole/manganese dioxide composites exhibited enhanced performance compared to that of the pure manganese dioxide [7]. Moreover, nanostructured conducting Ppy/MnO₂ with high surface area and porosity gives excellent performance in energy storage devices because of their unique characteristic properties of conducting pathways, surface interactions and nanoscale dimensions [6–8]. There are many methods available in the literature for the preparation of Ppy/MnO₂ nanocomposites including chemical and electrochemical synthetic routes. Among these preparation methods, simple redox reaction in aqueous mediated reactions gains interest due to its simple, low-cost, environmental friendly, large-scale production. To the best of the author's knowledge, there are rare reports on AC conductivity studies on polypyrrole/manganese dioxide nanocomposites.

In the present study, an attempt has been made to prepare MnO₂ and Ppy/MnO₂ nanocomposites using simple reducing agents such as ethylene glycol and pyrrole, respectively. The prepared samples are subjected to AC conductivity measurement studies. The results show that the sample Ppy/MnO₂ nanocomposite exhibits better conductivity than that of the pure MnO₂ nanostructures. The better conductivity may be due to the presence of polypyrrole polymer backbone which provided a conducting support to the poor conducting MnO₂ nanostructures.

2 Experimental

2.1 Preparation of manganese dioxide nanostructures and polypyrrole/manganese dioxide nanocomposite

All chemicals used were of analytical grade and they were used as received. The schematic preparation diagram is as shown in Fig. 1. Herein, we adopted a simple synthetic procedure for the preparation of desired materials which involves a simple reduction–oxidation reaction at ambient conditions [4, 7]. We used simple organic reducing agents such as ethylene glycol and pyrrole to reduce KMnO₄ to MnO₂ and Ppy/MnO₂ nanocomposite respectively. In a typical preparation of manganese dioxide, 3.0 g of KMnO₄ was dissolved in 200 mL of distilled water [4]. To the above solution, 2 mL of ethylene glycol was added drop wise with stirring. After 30 min, a brown coloured precipitate of polyethylene glycol/MnO₂ nanocomposite was formed. The precipitate was washed several times using water followed by the ethanol. After repeated washing with water, polyethylene glycol in the nanocomposite can be removed easily as it is soluble in water. Finally, a brown coloured solid was separated and dried at 100 °C overnight.

For the preparation of polypyrrole/manganese dioxide, 3.0 g of KMnO₄ was dissolved in 200 mL of distilled water [7]. To this solution, 2 mL of pyrrole monomer was added upon stirring and continued stirring for about 30 min. A black coloured precipitate of Ppy/MnO₂ nanocomposite was formed and the precipitate was washed with a large amount of distilled water several times followed by ethanol. After washing with the water several times, the Ppy/MnO₂ nanocomposite remains same as it is not soluble in water. Finally, the separated solid was dried at 100 °C overnight. The prepared manganese dioxide and polypyrrole/manganese dioxide nanostructure materials are used for physicochemical characterization, AC conductivity and dielectric measurements.

2.2 Characterization methods

Powder X-ray diffraction (XRD) patterns of the precursor and the final products were recorded using Bruker D8 advance diffractometer with

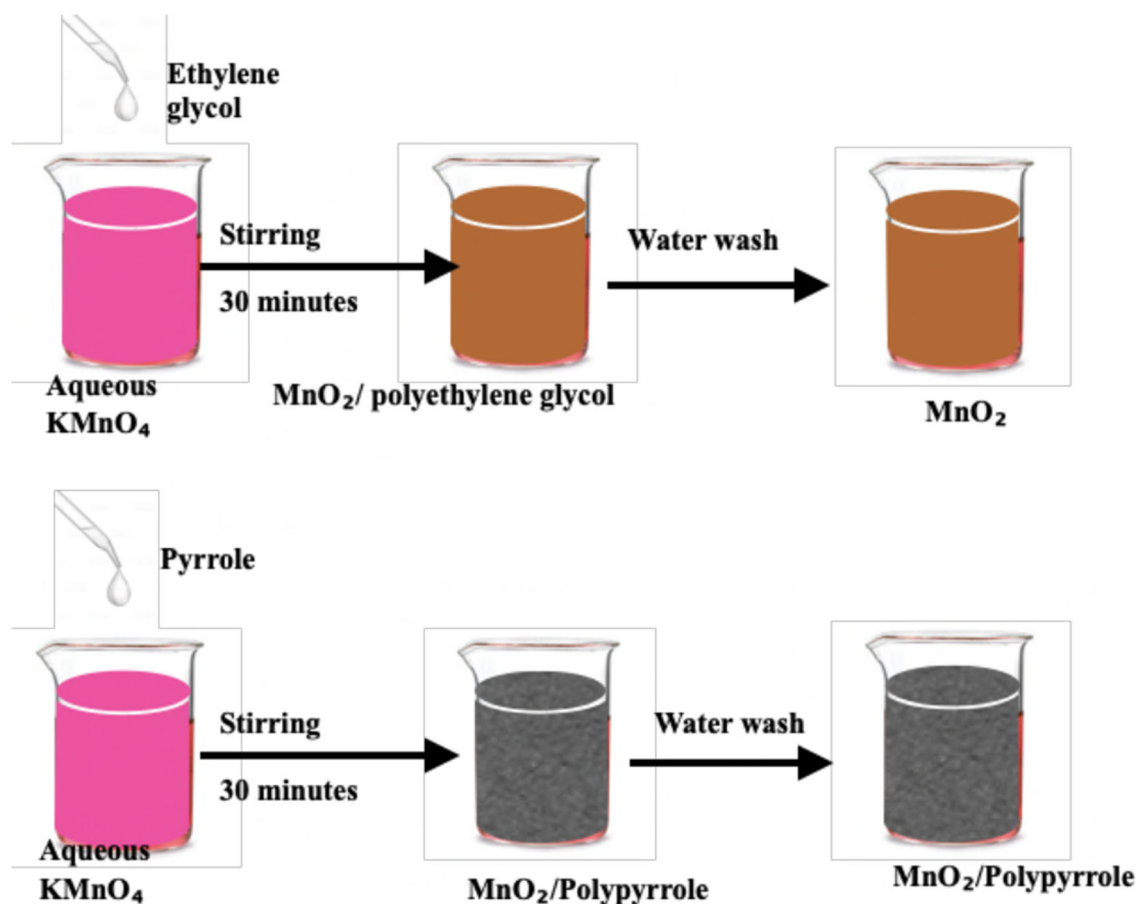


Fig. 1 Schematic preparation diagram pure MnO_2 and Ppy/ MnO_2 composite nanostructures

monochromatized $\text{Cu K}\alpha$ ($\lambda = 1.5418 \text{ \AA}$) incident radiation as the source. Infrared absorption spectrum was recorded in a FT-IR spectrum 1000 PERKIN ELMER spectrometer on dried sample using KBr pellet. The microscopy studies were conducted by using scanning electron microscopy (SEM, FEI Co. model Sirion) equipped with energy dispersive X-ray (EDX). AC conductivity and dielectric properties of the sample were carried out using Agilent 4294A.

2.3 Preparation of electrodes and AC conductivity measurements

The room temperature AC conductivity measurements of the prepared samples are examined using Agilent 4294A precision impedance analyser in the frequency range 10 Hz to 100 MHz. A variable frequency signal source section generates the test signal, applied to the material being investigated. For impedance measurements, the samples were prepared in sandwich geometry with size of 10 mm in

diameter and thickness of 1 mm coated on both sides with silver. The silver-coated surface contacts were drawn for measurements by using fine enamelled copper wire of 38 AWG (0.1 mm diameter) and conductive silver paint.

3 Results and discussion

To explore the structure and phase purity of the prepared samples, the samples were characterized using powder X-ray diffraction (PXRD). The XRD patterns of the as-prepared samples of pure MnO_2 and Ppy/ MnO_2 nanocomposite are presented in Fig. 2. The PXRD pattern shows only one asymmetric broad peak at 37.5° (2θ) indicating MnO_2 nanostructure reveals the amorphous structure. This peak corresponds to the main peak of the α - MnO_2 cryptomelane [6]. The other PXRD pattern belongs to Ppy/ MnO_2 nanocomposite prepared using pyrrole as a reducing agent exhibits one asymmetric broad peak

at 37.5° (2θ) indicating MnO_2 nanostructure reveals the amorphous structure [6, 7]. Along with MnO_2 nanostructure PXRD peak, there is one more broad peak at 25.5° (2θ) which corresponds to polypyrrole present in the nanocomposite confirming the presence of polypyrrole in Ppy/ MnO_2 nanocomposite.

The chemical structure and functional groups of MnO_2 and Ppy/ MnO_2 samples were further analysed using FT-IR spectrometer and the recorded spectra are presented in Fig. 3. In Fig. 3a, two distinct peaks at 742 cm^{-1} and 500 cm^{-1} are observed and these peaks are assigned to the Mn–O stretching vibrations of $[\text{MnO}_6]$ octahedral in MnO_2 [5, 6]. The peak around 3400 cm^{-1} which corresponds to –OH stretching vibrations observed is corresponding to the water molecule present in amorphous MnO_2 . In Fig. 3b, the peak 1538 cm^{-1} is designated to the vibrations of C=C/C–C, while the bands at 1415 cm^{-1} and 1340 cm^{-1} are assigned to the pyrrole ring vibration [7]. The bands at 1290 cm^{-1} and 1153 cm^{-1} are assigned to the C–H in-plane deformation and the C–N stretching vibrations, while other bands at 1017 cm^{-1} and 967 cm^{-1} reflect the existence of N–H in-plane deformation vibration and the C–H out-of-plane vibration, respectively, implying the doping state of polypyrrole [7]. Further, the two distinct peaks at 742 cm^{-1} and 515 cm^{-1} can be readily attributed to the Mn–O stretching vibrations

of $[\text{MnO}_6]$ octahedral in Ppy/ MnO_2 composite [6, 7]. Besides, the peak around 3400 cm^{-1} corresponds to –OH stretching vibrations observed and it is attributed to water molecule present in the Ppy/ MnO_2 sample.

To investigate the morphological evidences of the heterostructures, samples were subjected to scanning electron microscopy (SEM). The typical SEM images of both pure MnO_2 and Ppy/ MnO_2 nanocomposite samples (Fig. 4a, b) are spongy in nature without clear boundary of particles. This is due to amorphous nature of the material, which is reflected in the XRD pattern (Fig. 2). It can be clearly seen that there are MnO_2 nanoparticles present in Ppy/ MnO_2 nanocomposite as shown in Fig. 4b. Further, the EDX analysis is conducted to examine the chemical composition of pure MnO_2 and Ppy/ MnO_2 nanocomposite samples as shown in Fig. 4c, d in which C, Mn and O elements were detected. There is a negligible C element found in case of pure MnO_2 (Fig. 4c) and considerable amount of C element with a carbon prominent peak is observed in case of Ppy/ MnO_2 composite (Fig. 4c). It further confirms the presence of more C from Ppy present in Ppy/ MnO_2 nanocomposite than that of the pure MnO_2 .

3.1 Conductivity studies

The variation of AC conductivity with frequency for pure MnO_2 and Ppy/ MnO_2 nanocomposite is as

Fig. 2 PXRD patterns of pure MnO_2 and Ppy/ MnO_2 composite nanostructures

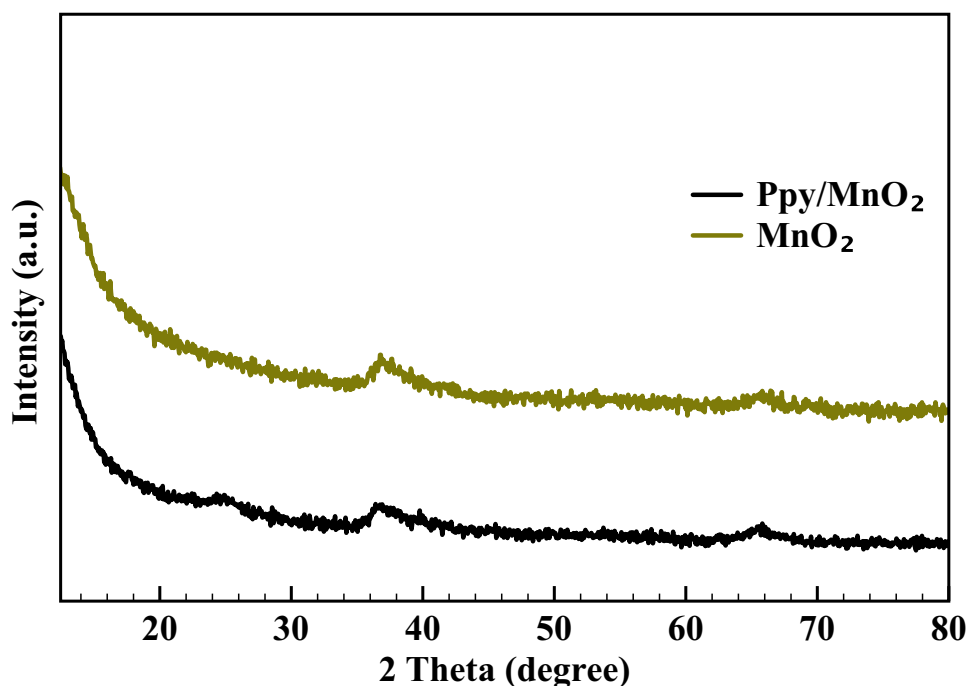
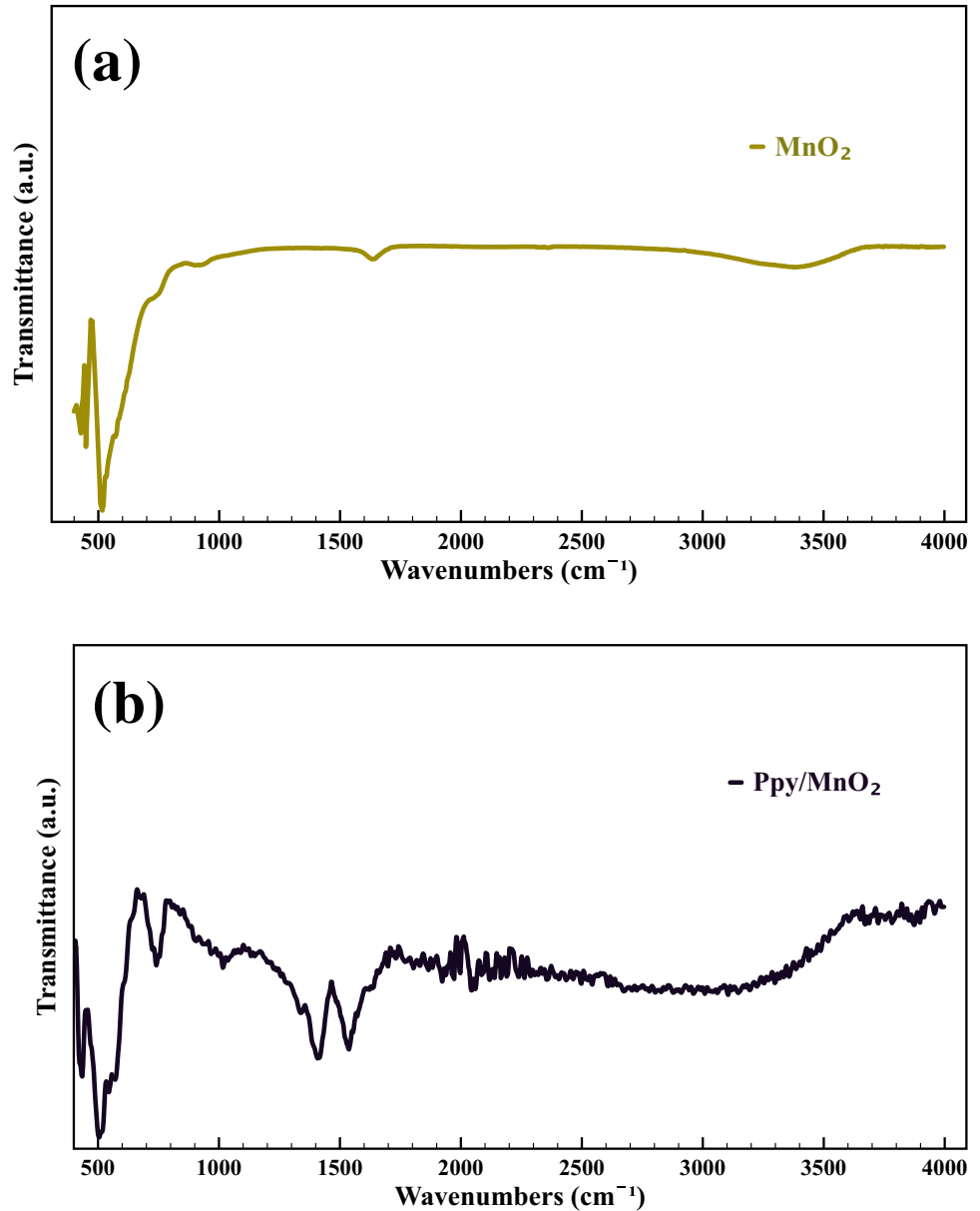


Fig. 3 FT-IR spectrum of pure MnO_2 and Ppy/ MnO_2 composite nanostructures



shown in Fig. 5. It is observed that AC conductivity of both the samples remains same up to 50 kHz, gradually increased up to 10 MHz and drastically increased at higher frequencies. The increase in AC conductivity at higher frequencies was observed for Ppy/ MnO_2 nanocomposite due to the presence of hopping charge carrier movement in the amorphous regions which are moving shorter distances in the polymer chain [9–11, 17]. It is observed from the figure that the conductivity of Ppy/ MnO_2 nanocomposite and MnO_2 remains constant up to 100 kHz. Thereafter, the conductivity of Ppy/ MnO_2 increased

which is a characteristic feature of disordered materials [11, 17]. At high frequencies, the AC conductivity increased due to the electronic charge motion in the amorphous region in Ppy/ MnO_2 nanocomposite.

Figure 6 represents the variation of real part of impedance (Z') as a function of frequency at room temperature. The pattern shows the variation as a function of frequency in the low-frequency region followed by the saturation region in the high-frequency region. This suggests the presence of hopping charge carrier behaviour in the material, such as electronic, dipolar and orientation polarization

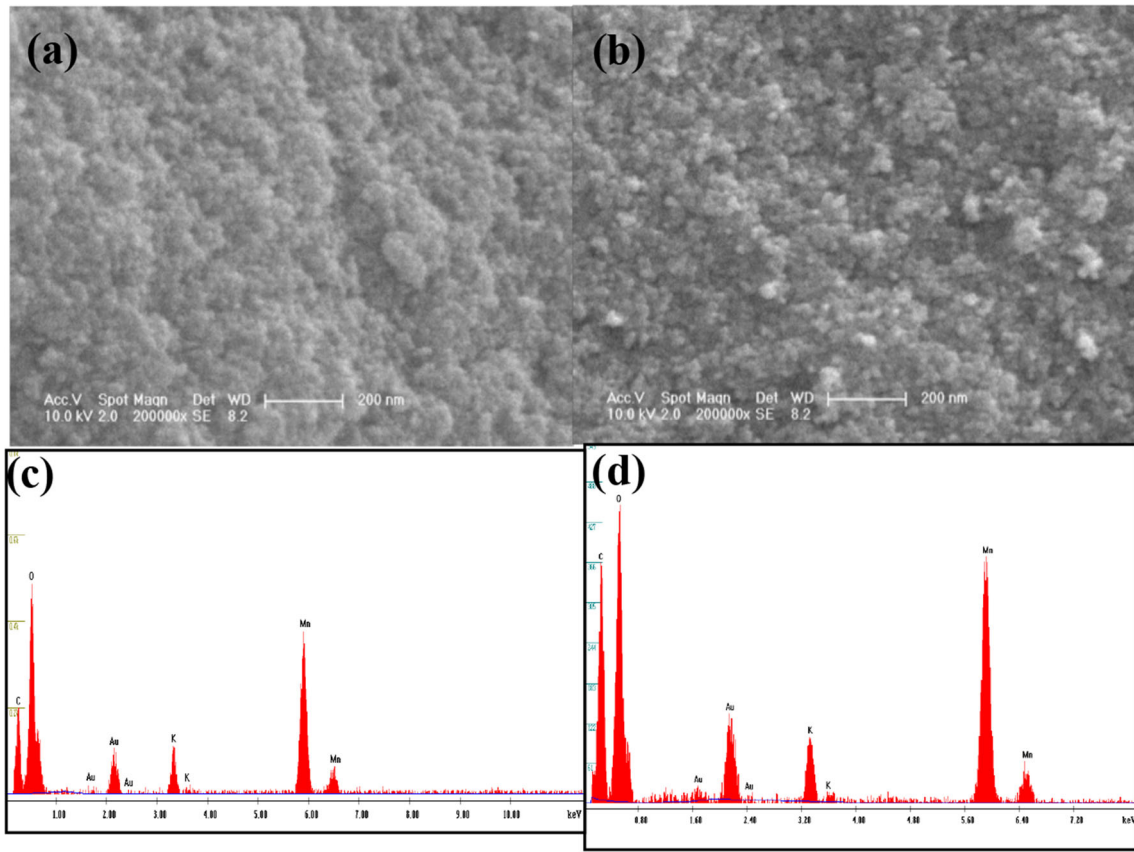


Fig. 4 SEM micrographs (a, b) and EDX patterns (c, d) of pure MnO₂ and Ppy/MnO₂ composite nanostructures

Fig. 5 AC conductivity measurement of pure MnO₂ and Ppy/MnO₂ composite nanostructures

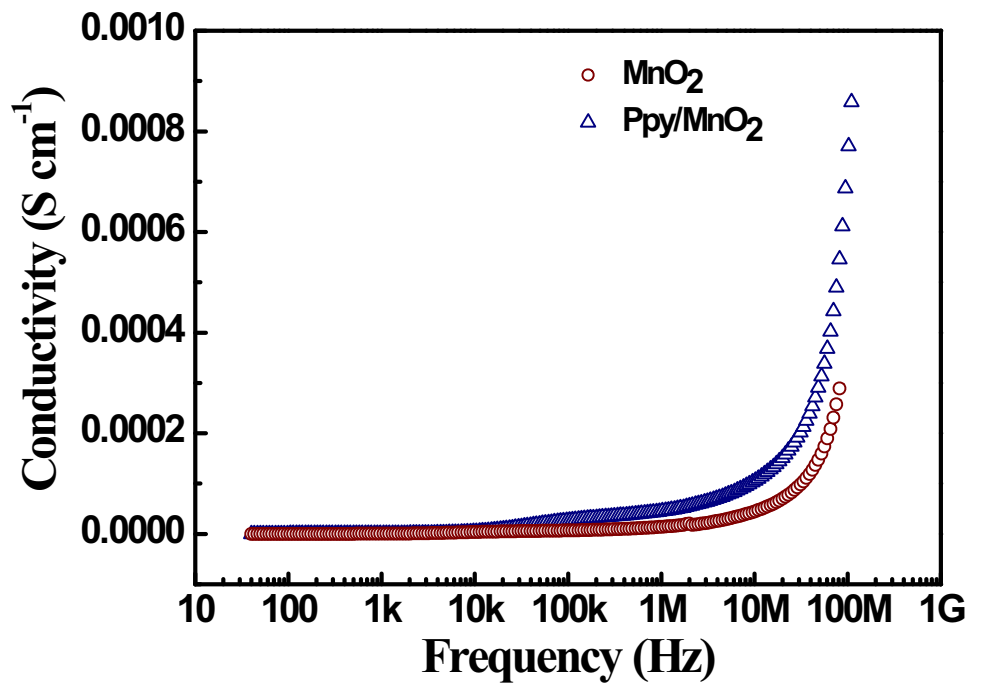


Fig. 6 Real part of impedance vs frequency measurement of pure MnO₂ and Ppy/MnO₂ composite nanostructures

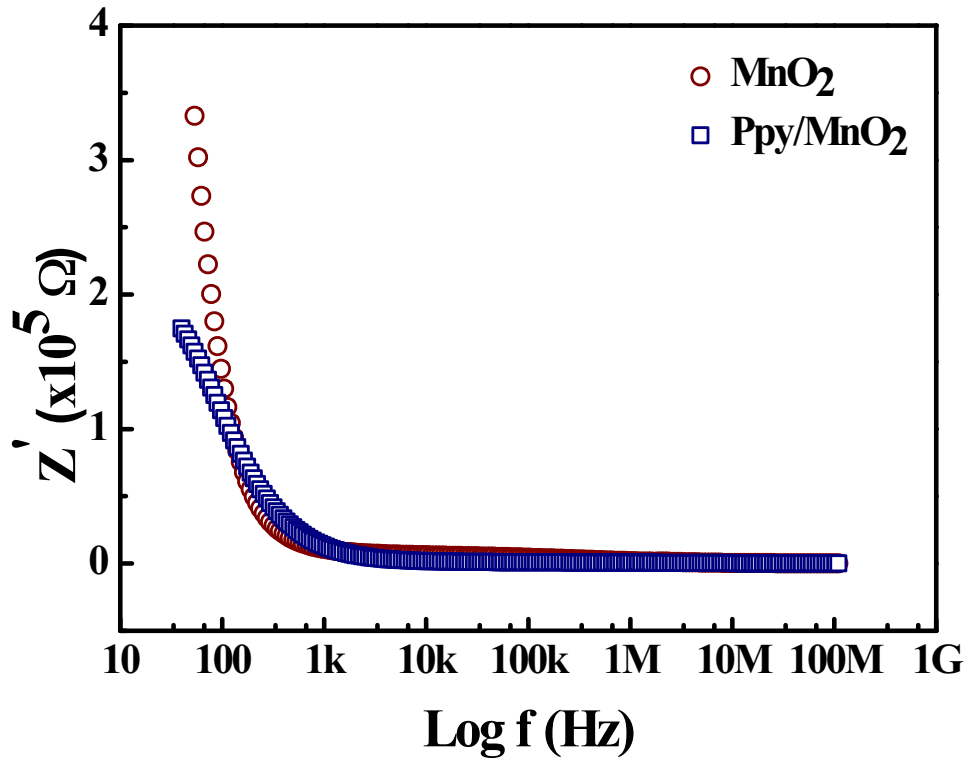
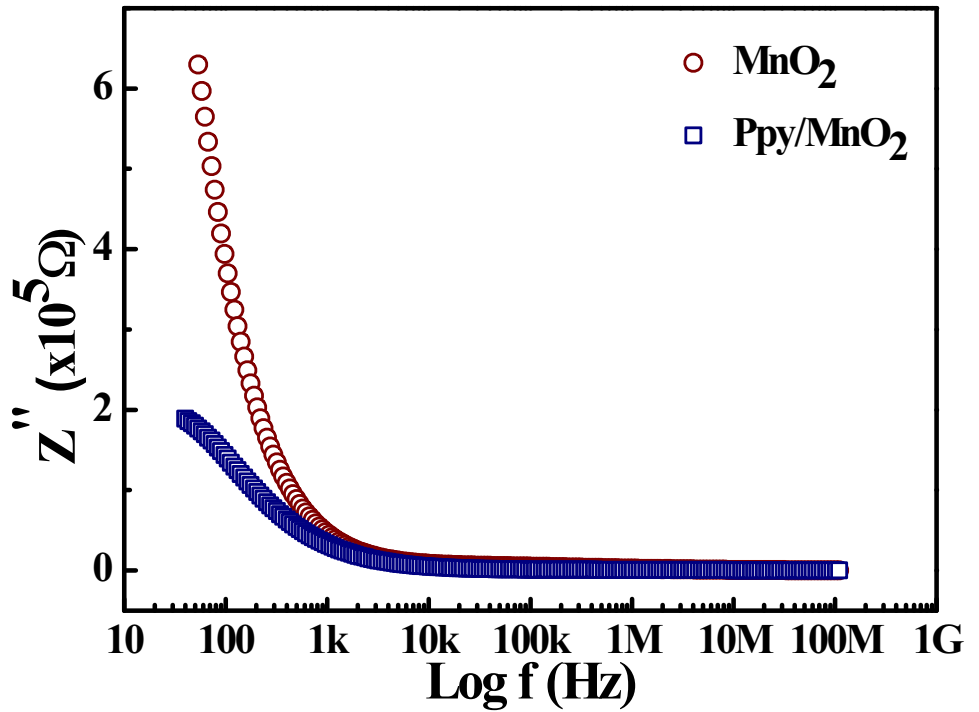


Fig. 7 Imaginary part of impedance vs frequency measurement of pure MnO₂ and Ppy/MnO₂ composite nanostructures



[9, 11, 17]. Further, it is observed that the resistance of the pure MnO₂ is more than that of Ppy/MnO₂ suggests that the as-prepared Ppy/MnO₂ nanocomposite

is more conductive than the pure MnO₂ nanostructures.

Fig. 8 Complex impedance spectra of pure MnO_2 and Ppy/ MnO_2 composite nanostructures

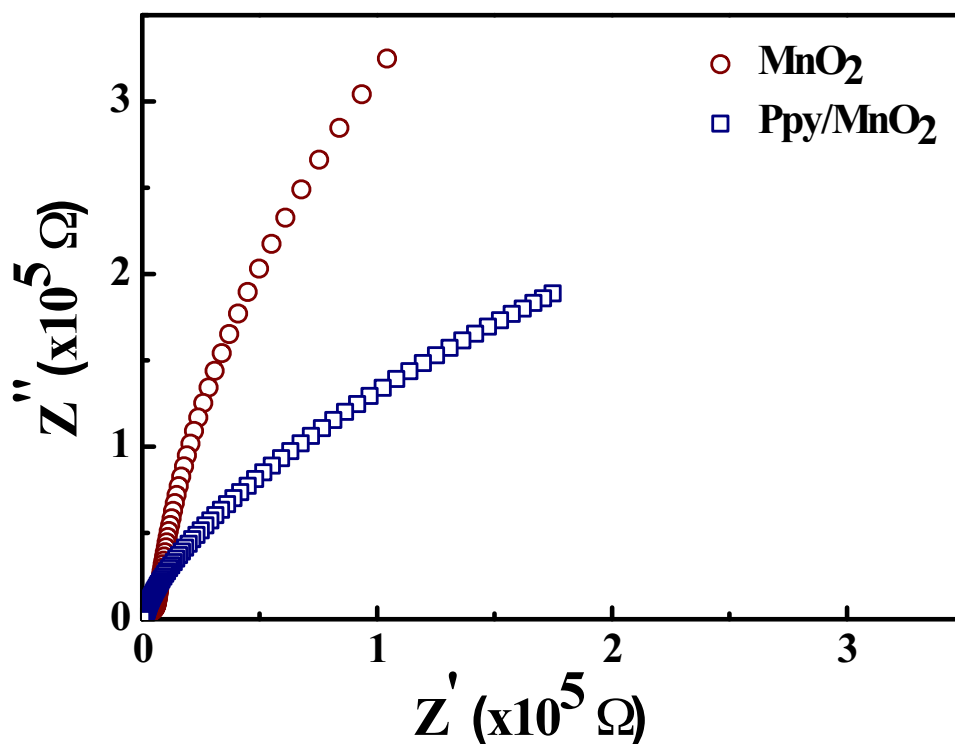


Figure 7 presents the variation of imaginary part of impedance (Z'') as a function of frequency. The imaginary part of impedance (Z'') decreases with the increase of frequency in both the cases. The higher electrical resistance of pure MnO_2 may be due the absence of the Ppy polymer chain [15, 18]. In Ppy/ MnO_2 , the Ppy facilitates the electronic charge carrier motion and hence the resistance decreased.

The complex impedance analysis is another approach to examine electrical properties of the material and it is shown in Fig. 8. The resistive nature of the sample with semicircular arcs was seen. The X-axis represents the real part, while Y-axis shows the imaginary part of the Nyquist plot. It is clearly observed from the Nyquist plot that the contribution of Ppy polymer chain enhances the conductivity in Ppy/ MnO_2 nanocomposite. The smaller semicircular arc indicates the more charge transfer in the presence of Ppy polymer chain in Ppy/ MnO_2 nanocomposite than that of the pure MnO_2 . It is clear from the impedance spectra that due to presence of hopping charge carriers in Ppy/ MnO_2 nanocomposite the conductivity is increased. On the other hand, minimum resistance of the Ppy/ MnO_2 composite is associated with the presence of conducting Ppy polymer chain [15–18].

4 Conclusions

Nanostructured Ppy/ MnO_2 nanocomposite was successfully prepared using pyrrole monomer as a reducing agent under ambient conditions. There was a notable change in the electrical conductivity properties for the sample Ppy/ MnO_2 and pure MnO_2 was observed. The AC electrical conductivity of Ppy/ MnO_2 is found to be more than the pure MnO_2 . The conductivity of Ppy/ MnO_2 nanocomposite increased as a function of frequency increased. The high electrical conductivity of Ppy/ MnO_2 nanocomposite is due to the movement of hopping charge carriers present in conducting polymer support to the MnO_2 . As the synthetic route is simple and low cost, this method can be adopted for the preparation of Ppy/ MnO_2 nanocomposite in large scale.

References

1. D.R. Rolison, R.W. Long, J.C. Lytle, A.E. Fischer, C.P. Rhodes, T.M. McEvoy, M.E. Bourga, A.M. Lubers, *Chem. Soc. Rev.* **38**, 226–252 (2009)
2. L.L. Zhang, X.S. Zhao, *Chem. Soc. Rev.* **38**, 2520–2531 (2009)

3. C. Li, H. Bai, G. Shi, *Chem Soc. Rev.* **38**, 2397–2409 (2009)
4. P. Ragupathy, D.H. Park, G. Campet, H.N. Vasan, S.J. Hwang, J.H. Choy, N. Munichandraiah, *J. Phys. Chem. C* **113**, 6303–6309 (2009)
5. S. Devaraj, N. Munichandraiah, *J. Phys. Chem. C* **112**, 4406–4417 (2008)
6. P. Ragupathy, H.N. Vasan, N. Munichandraiah, *J. Electrochem. Soc.* **155**, A34–A40 (2008)
7. S. Shivakumara, N. Munichandraiah, *J. Alloys Compd.* **787**, 1044–1050 (2019)
8. V.C. Lokhande, A.C. Lokhande, C.D. Lokhande, J.H. Kim, T. Ji, *J. Alloys Compd.* **682**, 381–402 (2016)
9. E. Kumar, S.C. Vella durai, L. Guru Prasad, D. Muthuraj, V. Bena Jothy, *J. Mater. Environ. Sci.* **8**, 3490–3495 (2017)
10. A. Vijayamari, K. Sadayandi, S. Sagadevan, P. Singh, *J. Mater. Sci.* **28**, 2739–2746 (2017)
11. K.M. Racik, K.P. Prabakaran, J. Madhavan, M. Victor Antony Raj, *Mater. Today* **8**, 162–168 (2019)
12. R.E. John, A. Chandran, M. Samuel, M. Thomas, K.C. George, *Physica E* **116**, 113720 (2020)
13. S. Palsaniya, H.B. Nemade, A.K. Dasmahapatra, *Carbon* **150**, 179–190 (2019)
14. H. Khan, K. Malook, M. Shah, *J. Mater. Sci.* **29**, 1990–1998 (2018)
15. J. Aguilar-Hernandez, K. Potje-Kamloth, *J. Phys. D* **34**, 1700–1711 (2001)
16. S. Capaccioli, M. Lucchesi, P.A. Rolla, G. Ruggeri, *J. Phys.* **10**, 5595–5617 (1998)
17. Y.A. Kulakarni, M.R. Jagadeesh, S. Jambaladinni, H.M. Suresh Kumar, M.S. Vasanthkumar, S. Shivakumara, *J. Mater. Sci.* **31**, 7226–7231 (2020)
18. E. Veena Gopalan, K.A. Malini, S. Saravanan, D. Sakthi Kumar, Y. Yoshida, M.R. Anantharaman, *J. Phys. D* **41**, 185005 (2008)

Publisher's Note Springer Nature remains neutral with regard to jurisdictional claims in published maps and institutional affiliations.